Cold Spring Harbor Protocols

Two-Photon Targeted Patching and Electroporation In Vivo

Michael Häusser and Troy W. Margrie

Email Alerting Service	Receive free email alerts when new articles cite this article - **click here.**
Subject Categories	Browse articles on similar topics from *Cold Spring Harbor Protocols.* Cell Imaging (459 articles) DNA Delivery/Gene Transfer (224 articles) DNA Delivery/Gene Transfer, general (261 articles) Electrophysiology (51 articles) Imaging for Neuroscience (259 articles) In Vivo Imaging (269 articles) In Vivo Imaging, general (134 articles) Multi-Photon Microscopy (80 articles) Patch Clamping (31 articles)

Two-Photon Targeted Patching and Electroporation In Vivo

Michael Häusser and Troy W. Margrie

By combining patch-clamp methods with two-photon microscopy, it is possible to target recordings to specific classes of neurons in vivo. Here we describe methods for imaging and recording from the soma and dendrites of neurons identified using genetically encoded probes such as green fluorescent protein (GFP) or functional indicators such as Oregon Green BAPTA-1. Two-photon targeted patching can also be adapted for use with wild-type brains by perfusing the extracellular space with a membrane-impermeable dye to visualize the cells by their negative image and target them for electrical recordings, a technique termed "shadowpatching." We discuss how these approaches can be adapted for single-cell electroporation to manipulate specific cells genetically. These approaches thus permit the recording and manipulation of rare genetically, morphologically, and functionally distinct subsets of neurons in the intact nervous system.

MATERIALS

It is essential that you consult the appropriate Material Safety Data Sheets and your institution's Environmental Health and Safety Office for proper handling of equipment and hazardous material used in this protocol.

RECIPE: Please see the end of this protocol for recipes indicated by <R>. Additional recipes can be found online at http://cshprotocols.cshlp.org/site/recipes.

Reagents

Biological sample

The animal (typically a rat or transgenic mouse) must be anesthetized and maintained according to the appropriate local and national ethical guidelines. The animal's head should be secured using a stereotaxic frame or a custom head mount (e.g., Judkewitz et al. 2009).

Cyanoacrylate glue (or dental acrylic)

Fluorescent dye (choose according to study of interest; see Step 2)

Internal recording solution for targeted patching <R>

The same pipette solution can be used for electroporation. Alternatively, HEPES-buffered artificial cerebrospinal fluid or phosphate-buffered saline containing 50 μM Alexa 594 can also be used.

Ketamine/xylazine mixture (used as anesthetic; Sigma-Aldrich)

Equipment

Analog-to-digital (A-D) converter (Instrutech)

Electroporation device (e.g., Axoporator 800A; Molecular Devices)

Motorized x–y–z micromanipulator (e.g., Luigs & Neumann)

Pipette puller (e.g., from Narishige or Sutter)

Stereotaxic frame

Cite this protocol as *Cold Spring Harb Protoc*; doi:10.1101/pdb.prot080143

Temperature controller (FHC)

Two-photon microscope for in vivo imaging

This can be a commercial instrument (e.g., from Sutter Instruments or Prairie Technologies) or a custom-made design (e.g., see Tsai et al. 2002), and it requires a mode-locked Ti:sapphire laser (e.g., Coherent or Spectra-Physics).

Voltage/current amplifier (e.g., MultiClamp 700B; Molecular Devices)

Water-immersion, high-numerical-aperture (NA) objective (e.g., 40×, 0.8-NA Nikon)

METHOD

1. Place the anesthetized animal in a stereotaxic frame, and perform the craniotomy according to standard surgical procedures used for in vivo patch-clamp preparations. Because optical clarity is essential, it is imperative that little or no bleeding occurs in the region where imaging and targeted patching will be performed. Before attaching the head plate used for stabilization, allow the skull to dehydrate to ensure robust fixation of the head plate (Fig. 1). Apply either cyanoacrylate glue or dental acrylic to the skull and gently fix the head plate.

   This step may also be performed in reverse; that is, the craniotomy can be created through the center hole of the head plate once it is fixed to the cranium. This has the advantages that it negates the need for the stereotaxic frame, fixative cannot leak into the craniotomy, and it reduces the overall preparation time.

   For many preparations, removal of the dura is essential to prevent the pipette from clogging as it enters the brain. However, in mice it is not always necessary.

2. To visualize electrodes, fill patch pipettes with internal recording solution containing a fluorescent dye (e.g., Alexa 594) or other indicator that can be clearly distinguished from the reporter probe (e.g., GFP) based on their different emission spectra (Fig. 1).
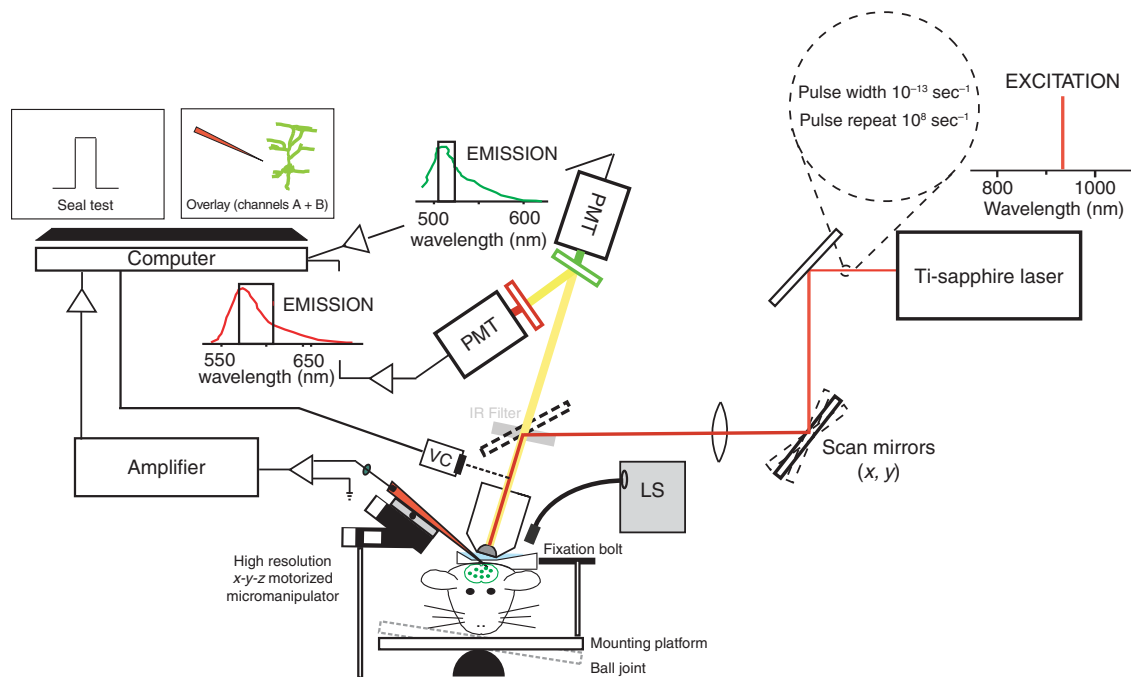

FIGURE 1. Schematic of the imaging setup for the targeted recording approach. Neurons are visualized using a two-photon microscope operated in conjunction with a mode-locked Ti:sapphire laser. Dual-channel detection is used to collect emitted light selected by an interference filter for monitoring the signals from Alexa 594 (the pipette; 610/BP40) and enhanced green fluorescent protein (eGFP) (expressed by the targeted cell type; 520/BP30). Under high magnification, water-immersion conditions can be achieved by loading the imaging window of the head-plate chamber (which is fixed to the cranium) with Ringer's solution. For added ease of use, the stereotaxic platform may be fixed to an x−y table or a ball-and-socket mounting plate.

3. While illuminating the cortical surface with an external light source, coarsely position the pipette over the region of interest using a low-power objective (4×–20×) under either video guidance or visualization via the binocular tube (Fig. 1). Guide the patch pipette to the center of the field of view, near the cortical region of interest, such that the forward diagonal motion (see Step 6) will place the pipette in the center of the region of interest.

4. Replace the low-power objective with the water-immersion, high-NA objective that is needed for targeted recordings (Fig. 1). Now, using two-photon excitation, visualize the dye-filled patch pipette. While the pipette is in the bath above the preparation, apply low positive pressure (20–40 mbar) to eject a bright plume of fluorescent dye from the pipette. Next, position the pipette just over the surface of the brain. If the dura is intact, its bright autofluorescence can be used to easily locate the correct depth. Apply a higher positive pressure (200–400 mbar) and enter the brain by moving the pipette in a diagonal motion. Once the pipette has cleanly entered the brain, with or without the dura, dye should be flowing freely out of the tip. Quickly reduce the positive pressure back to 20–40 mbar to prevent increasing the background fluorescence level in the neuropil.

   Note that a single low-power, high-NA objective can be used for both Steps 3 and 4.

5. Find a cell that is suitable for targeting.

   This can be done by visualizing GFP-positive neurons in transgenic animals (or by virally transfecting neurons to express GFP) (Dittgen et al. 2004). Alternatively, ejection of Alexa dye from the patch pipette into the extracellular space in wild-type brains can be used to visualize neurons via the "negative image" of the unfilled cells (Fig. 2; Kitamura et al. 2008).

6. Once the cell has been selected, position it in the center of the field of view. Determine the depth of the cell from the surface of the brain, then retract the pipette from the craniotomy by a known distance and lower the manipulator in the *z*-axis according to the distance of the cell from the brain surface.

   For successful navigation of the patch pipette toward GFP-labeled cells, it is helpful to overlay the two emission channels (Fig. 1).

7. In voltage-clamp mode, move the pipette rapidly down toward the cell while monitoring the tip resistance using a test pulse. Moving the pipette back along the diagonal axis, position it inside the brain to ∼50–100 µm from the cell of interest.

   A plume of fluorescent dye around the pipette tip should be observed—this is a good sign, as it indicates that the electrode tip has not been clogged or obstructed.

8. When approaching the cell, reduce the positive pressure to ∼20–40 mbar to reduce the background fluorescence, ensuring that the pipette resistance remains constant. Verify this using both optical and electrical readouts (see Fig. 1).
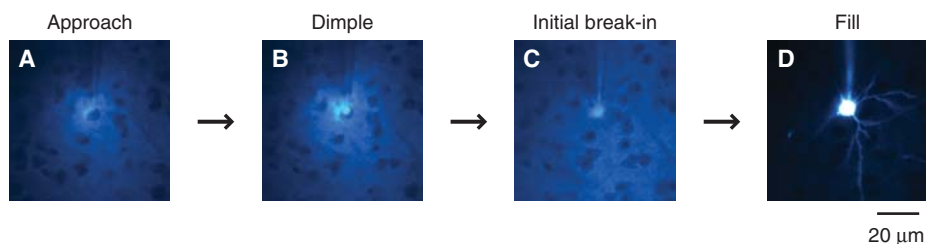

FIGURE 2. Shadowpatching of unlabeled cells in vivo using two-photon microscopy. (*A*) A water-soluble, low-molecular-weight dye is included in the pipette solution and fills the neuropil without entering cell bodies, which consequently appear as dark shadows. This way, morphological cues can be used to target recordings and the pipette can be optimally positioned for gigaseal formation. (*B*) Once a dimple forms in the surface of the cell (a layer 2/3 pyramidal neuron 150 µm deep in mouse visual cortex), it is immediately clear in the image, and standard procedures are used to establish the whole-cell patch-clamp configuration. After releasing positive pressure, the dye in the neuropil quickly diffuses away. (*C*) Following break-in, the cell begins to fill with dye and the neuropil continues to fade. (*D*) Low series resistance whole-cell recordings permit rapid dialysis with pipette solution, showed here by a bright fill. (S Smith, unpubl.)

If >20–40 mbar of pressure is required to observe a plume out of the pipette tip, then the tip may be clogged, even if little to no increase in tip impedance is observed.

9. Navigate toward the target cell while monitoring the electrode resistance continuously. Lateral excursions of the pipette are feasible, but should be limited to <50 μm. Position the electrode tip in a focal plane ∼5–10 μm directly away from the cell. While visually tracking the tip and monitoring the electrode resistance simultaneously, move toward the center of the cell body. This may be done by either moving along the diagonal axis or by positioning the tip directly above the center of the cell and moving vertically.

   Note that once the tip of the electrode comes into contact with the cell membrane, the resistance of the pipette will increase and the seal test amplitude will fluctuate at heartbeat frequencies (Margrie et al. 2002). In some instances, contact with the cell can been recognized via a dimple in the cell membrane (Fig. 2).

10. Remove the positive pressure and take the command potential to −70 mV. Some slight negative pressure may be required to achieve gigaohm seal formation. This can take from 5–10 sec up to 1 min. Noninvasive recordings of activity by recording cell-attached spikes can be performed at this point. If seal formation fails, change the pipette; the same cell may be attempted more than once. In cell-attached mode, increase the test pulse amplitude and apply a slow ramp of negative pressure to obtain the whole-cell configuration.

11. Verify that targeting is successful using two different approaches.

    i. Electrophysiologically: Verify resting membrane potential, assess access resistance, and determine the firing properties.

    ii. Optically: Observe filling of the target cell with dye (Figs. 2 and 3), and when targeting GFP-positive neurons, observe initial mixing of the GFP and dye signals, followed by a gradual washout of GFP signal and replacement with the internal dye.

12. This approach can be adapted for electroporation of dye or DNA into selected neurons, which should be included in the pipette solution. At Step 10, release the positive pressure and apply a train of voltage pulses (e.g., 50 square −12-V pulses of 0.5 msec duration at 50 Hz works well for layer 2/3 cortical neurons) via the electroporation device. Juxtacellular (or loose cell-attached) recordings of spontaneous or stimulus-evoked spikes can be made before the electroporation to characterize the targeted cell functionally. Successful electroporation can be visualized directly via the Alexa 594 included in the pipette solution by monitoring its injection into the cell, and subsequently by imaging expression of GFP (if plasmid DNA for GFP is also included in the pipette) (Fig. 4).
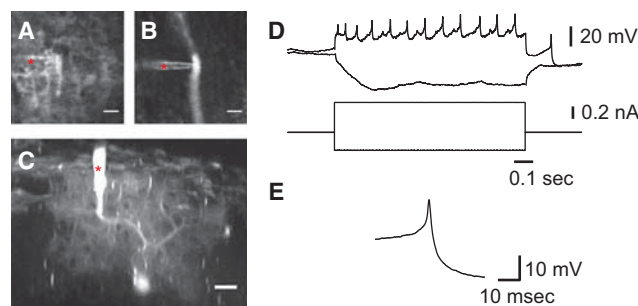

FIGURE 3. Targeted dendritic recording from cerebellar Purkinje cell in vivo. (*A*) Individual dendrites can be visualized using the shadow imaging technique. Red dot indicates the patch pipette. Scale bar, 5 μm. (*B*) Following break-in, the targeted dendrite is filled with dye. (*C*) *x − z* projection image of the entire cell after filling. Scale bar, 20 μm. (*D*) Voltage responses to current pulses (−0.3 and 0.9 nA). (*E*) Enlarged waveform of a simple spike at the dendritic recording site. (K Kitamura, unpubl.)
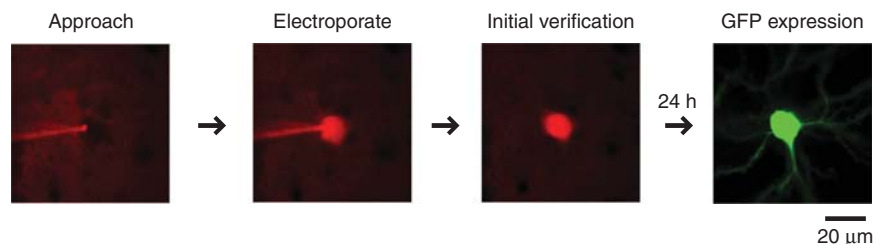
FIGURE 4. Targeted electroporation in vivo. Negative contrast image of a mouse neocortical layer 2/3 pyramidal neuron before electroporation, during electroporation, and a few minutes after electroporation (filled with Alexa 594). On the far *right* is an image of the same neuron taken 24 h later, showing bright eGFP fluorescence throughout the dendritic tree. Scale bar, 20 µm. (B Judkewitz, unpubl.)

DISCUSSION

Whole-cell recordings are useful for recording synaptic and spiking activity of neurons in vivo because the formation of a high-resistance seal between pipette and membrane ensures stable recordings for prolonged periods and is an approach that can even be used in awake, head-fixed, or behaving animals (Margrie et al. 2002; Lee et al. 2006). However, "blind" (i.e., nontargeted) recordings suffer from the problem that cell sampling is generally based on anatomical predominance, with the largest and/or the most numerous cell types being more readily sampled than the smallest or least abundant cells. This is, of course, dependent on the overall architecture of the brain area of interest, but in many regions that contain anatomically, genetically, and functionally diverse populations of neurons, such as the neocortex, reliable sampling has not been possible for many subtypes of cells. Targeted recordings from specific cells expressing a fluorescent marker are possible by combining in vivo two-photon microscopy (Denk et al. 1990; Svoboda et al. 1997) with the use of transgenic mice expressing GFP (Margrie et al. 2003) or viral vectors designed to drive expression via cell-specific promoters (Dittgen et al. 2004). Two-photon targeted patching can also be adapted for use with wild-type brains by shadow-patching, that is, filling the extracellular space with a nonpermeant dye to visualize the cells by their negative image (Kitamura et al. 2008). Furthermore, by prelabeling populations of neurons with a fluorescent Ca^{2+} indicator for action potential imaging (Stosiek et al. 2003; Garaschuk et al. 2006) or by expressing genetically encoded Ca^{2+} sensors, functionally defined neurons can be targeted for recording (Kerr et al. 2005; Greenberg et al. 2008; Wallace et al. 2008; Rochefort et al. 2009; Schultz et al. 2009; Tian et al. 2009; Lütcke et al. 2010). In vivo targeted electroporation of dyes (Nevian and Helmchen 2007) and DNA (Kitamura et al. 2008) is made possible by extracellular stimulation via patch pipettes targeted to individual cells.

Practical Considerations

- An outstanding preparation is crucial for successful targeted recordings. Any preparation that shows visible blood, edema, and/or pulsation can prevent adequate visualization of the cell, seal formation, and/or maintenance of the recording. Great care should be taken when performing craniotomies, removing dura, and mounting and securing recording chambers to minimize damage (for detailed procedures and troubleshooting tips, see Komai et al. 2006; Judkewitz et al. 2009).

- Brain movement must be rigorously minimized to maximize the stability of the preparation and duration of recordings. This can be achieved by covering the brain with 200 µL of 1.5% (w/v) agarose and a glass coverslip (optional) in conjunction with an appropriate chamber (e.g., see Judkewitz et al. 2009).

- Clogged or contaminated electrodes can prevent gigaohm seal formation. This should be avoided by rigorously filtering pipette solutions (both for storage and on day of use), ensuring that the

pipette enters the brain under high pressure, and verifying that a plume of solution is exiting the mouth of the pipette at all times. Clogged pipettes can sometimes be unclogged using a brief pulse of high pressure (>200 mbar), although this may dramatically raise background fluorescence in the tissue, limiting visibility.

- As in two-photon microscopy in general, laser illumination should be minimized, particularly during seal formation, which can be compromised by high laser powers (Komai et al. 2006). The laser power used should be the minimum consistent with adequate resolution of the pipette and targeted cell.

Examples of Applications

Targeted patch-clamp recordings have been used to make recordings from specific cell types in intact mammalian networks. For example, recordings have been targeted to genetically identified interneurons (Margrie et al. 2003; Liu et al. 2009) and genetically modified neurons labeled with GFP (Dittgen et al. 2004; Komai et al. 2006). Furthermore, this approach can be used to record from neurons that have been characterized functionally using synthetic (Greenberg et al. 2008; Rochefort et al. 2009; Schultz et al. 2009) or genetically encoded (Wallace et al. 2008) Ca^{2+} sensors. Such an approach is particularly valuable for calibration of Ca^{2+} signals in terms of the underlying temporal spiking patterns, which are notoriously difficult to extract quantitatively from Ca^{2+} signals alone and require sophisticated algorithms that must be optimized based on combined imaging and electrophysiological data (Yaksi and Friedrich 2006; Greenberg et al. 2008; Vogelstein et al. 2009).

One application that may prove to be particularly useful for the targeted approach is in vivo dendritic recording. There are only a few examples in the literature of "blind" recordings from dendrites in vivo (e.g., Llinas and Nicholson 1971; Helmchen et al. 1999; Larkum and Zhu 2002; Waters et al. 2003) owing in part to the small caliber of dendrites. As shown in Figure 3, it is possible using the targeted approach to make recordings directly from dendrites of visually identified neurons at defined locations in the dendritic tree (Kitamura et al. 2008). This approach may allow a more systematic investigation of the properties of dendrites in vivo.

Finally, using essentially the same approach, it is possible to electroporate visually and/or genetically identified neurons. This can be useful for injecting Ca^{2+} dyes into defined groups of neurons (Nevian and Helmchen 2007), providing more control over cell type and number than the use of genetically encoded or bulk-loaded indicators. Moreover, this approach can be used to genetically alter identified neurons via electroporation of plasmid DNA (Fig. 4; Kitamura et al. 2008; Judkewitz et al. 2009). This should allow the function of specific genes to be identified on the single-cell level in the absence of the more widespread deleterious effects normally associated with the use of transgenic mice or viral approaches. One of the great advantages of the single-cell electroporation approach is that it can be targeted to neurons identified by their functional profile by using the same electrode to make electrophysiological recordings from neurons before electroporation.

Advantages and Limitations

Targeted recording allows the experimenter to select the cell type to explore. Thus, with the use of GFP and the appropriate promoters, genetically defined cell types can be targeted for electrophysiological recordings. If neuronal types have a distinctive morphological signature or location (e.g., in specific cell layers), shadow patching can also be used to discriminate different cell types. Furthermore, the introduction or expression of activity-dependent probes (such as Ca^{2+} dyes) allows the functional signature of individual cells to be used as a criterion for targeting. Together, these approaches allow recordings to be targeted to rare or distinctive cell types based on their genetic, morphological, or functional signature, which would be extremely difficult or impossible using blind recording techniques.

M. Häusser and T.W. Margrie

The ability to visualize the cell before and during recording provides several additional advantages. First, cell properties can be assessed morphologically or functionally (using activity-dependent probes) before recording from the cell of interest. Second, the process of seal formation can be visualized directly: Not only can the position of the electrode on the cell be optimized (e.g., to allow dendritic recordings or target the pipette to the center of the soma), but dimple formation, often a valuable "signature" preceding an effective gigaohm seal, can be monitored and terminated at precisely the right moment before applying suction to form a seal. This can dramatically improve the success rates and quality of patch-clamp recordings. Third, the position of the electrode can be monitored during the recording and corrected, for example, for drift or movement. Finally, introduction of morphological markers or activity-dependent dyes via the patch pipette can allow morphology to be assessed in vivo during the experiment and also permit simultaneous measurement of electrical and chemical signaling in the same cell. Furthermore, it allows the experimenter to return to the same cell at later time points to assess changes in function following manipulations, either extrinsic or following genetic manipulation via electroporation (Kitamura et al. 2008).

The main limitation of the targeted approach, aside from requiring an expensive two-photon microscopy setup, is that it is limited to cells that can be visualized using two-photon microscopy. Currently this is possible down to a depth of up to ~1000 µm (Theer et al. 2003; Helmchen and Denk 2005; Theer and Denk 2006), which in principle allows targeted recording from most cortical layers in rodents but precludes targeting neurons in deeper brain structures. In the future, it may be possible to combine visualization of deep neurons, such as those in hippocampus, using microendoscopy (Jung et al. 2004) combined with patch-clamp recording, although this will require a strategy for positioning the patch pipette within the field of view of the microendoscope. Targeted patch-clamp recordings have also thus far been restricted to anesthetized, head-fixed animals. However, given recent progress in two-photon imaging from awake, head-fixed (Dombeck et al. 2007; Greenberg et al. 2008), and freely moving animals (Helmchen et al. 2001; Flusberg et al. 2005; Engelbrecht et al. 2008), as well as in patch-clamp recording from freely moving animals (Lee et al. 2006, 2009), one can envisage the possibility of targeted recordings from awake, head-fixed, and possibly even freely moving animals in the near future.

RECIPE

Internal Recording Solution for Targeted Patching

Reagent	Final concentration
Potassium gluconate	130 mM
Sodium gluconate	10 mM
HEPES	10 mM
Phosphocreatine	10 mM
MgATP	4 mM
GTP	0.3 mM
NaCl	4 mM
Biocytin (Sigma-Aldrich)	0.3%–1%
Alexa 594 (Molecular Probes)	0.06 mM

Adjust the pH to 7.2. Filter through a 0.45-µm syringe filter (Millipore) and store at −20°C.

ACKNOWLEDGMENTS

Cold Spring Harbor Protocols

www.cshprotocols.org

Cite this protocol as *Cold Spring Harb Protoc*; doi:10.1101/pdb.prot080143

REFERENCES

Denk W, Strickler JH, Webb WW. 1990. Two-photon laser scanning fluorescence microscopy. *Science* **248:** 73–76.

Dittgen T, Nimmerjahn A, Komai S, Licznerski P, Waters J, Margrie TW, Helmchen F, Denk W, Brecht M, Osten P. 2004. Lentivirus-based genetic manipulations of cortical neurons and their optical and electrophysiological monitoring in vivo. *Proc Natl Acad Sci* **101:** 18206–18211.

Dombeck DA, Khabbaz AN, Collman F, Adelman TL, Tank DW. 2007. Imaging large-scale neural activity with cellular resolution in awake, mobile mice. *Neuron* **56:** 43–57.

Engelbrecht CJ, Johnston RS, Seibel EJ, Helmchen F. 2008. Ultra-compact fiber-optic two-photon microscope for functional fluorescence imaging in vivo. *Opt Express* **16:** 5556–5564.

Flusberg BA, Jung JC, Cocker ED, Anderson EP, Schnitzer MJ. 2005. In vivo brain imaging using a portable 3.9 gram two-photon fluorescence microendoscope. *Opt Lett* **30:** 2272–2274.

Garaschuk O, Milos RI, Konnerth A. 2006. Targeted bulk-loading of fluorescent indicators for two-photon brain imaging in vivo. *Nat Protoc* **1:** 380–386.

Greenberg DS, Houweling AR, Kerr JN. 2008. Population imaging of ongoing neuronal activity in the visual cortex of awake rats. *Nat Neurosci* **11:** 749–751.

Helmchen F, Denk W. 2005. Deep tissue two-photon microscopy. *Nat Methods* **2:** 932–940.

Helmchen F, Svoboda K, Denk W, Tank DW. 1999. In vivo dendritic calcium dynamics in deep-layer cortical pyramidal neurons. *Nat Neurosci* **2:** 989–996.

Helmchen F, Fee MS, Tank DW, Denk W. 2001. A miniature head-mounted two-photon microscope. High-resolution brain imaging in freely moving animals. *Neuron* **31:** 903–912.

Judkewitz B, Rizzi M, Kitamura K, Häusser M. 2009. Targeted single-cell electroporation of mammalian neurons in vivo. *Nat Protoc* **4:** 862–869.

Jung JC, Mehta AD, Aksay E, Stepnoski R, Schnitzer MJ. 2004. In vivo mammalian brain imaging using one- and two-photon fluorescence microendoscopy. *J Neurophysiol* **92:** 3121–3133.

Kerr JN, Greenberg D, Helmchen F. 2005. Imaging input and output of neocortical networks in vivo. *Proc Natl Acad Sci* **102:** 14063–14068.

Kitamura K, Judkewitz B, Kano M, Denk W, Häusser M. 2008. Targeted patch-clamp recordings and single-cell electroporation of unlabeled neurons in vivo. *Nat Methods* **5:** 61–67.

Komai S, Denk W, Osten P, Brecht M, Margrie TW. 2006. Two-photon targeted patching (TPTP) in vivo. *Nat Protoc* **1:** 647–652.

Larkum ME, Zhu JJ. 2002. Signaling of layer 1 and whisker-evoked Ca^{2+} and Na^+ action potentials in distal and terminal dendrites of rat neocortical pyramidal neurons in vitro and in vivo. *J Neurosci* **22:** 6991–7005.

Lee AK, Manns ID, Sakmann B, Brecht M. 2006. Whole-cell recordings in freely moving rats. *Neuron* **51:** 399–407.

Lee AK, Epsztein J, Brecht M. 2009. Head-anchored whole-cell recordings in freely moving rats. *Nat Protoc* **4:** 385–392.

Liu BH, Li P, Li YT, Sun YJ, Yanagawa Y, Obata K, Zhang LI, Tao HW. 2009. Visual receptive field structure of cortical inhibitory neurons revealed by two-photon imaging guided recording. *J Neurosci* **29:** 10520–10532.

Llinas R, Nicholson C. 1971. Electrophysiological properties of dendrites and somata in alligator Purkinje cells. *J Neurophysiol* **34:** 532–551.

Lütcke H, Murayama M, Hahn T, Margolis DJ, Astori S, Zum Alten Borgloh SM, Göbel W, Yang Y, Tang W, Kügler S, et al. 2010. Optical recording of neuronal activity with a genetically-encoded calcium indicator in anesthetized and freely moving mice. *Front Neural Circuits* **4:** 9.

Margrie TW, Brecht M, Sakmann B. 2002. In vivo, low-resistance, whole-cell recordings from neurons in the anaesthetized and awake mammalian brain. *Pflügers Arch* **444:** 491–498.

Margrie TW, Meyer AH, Caputi A, Monyer H, Hasan MT, Schaefer AT, Denk W, Brecht M. 2003. Targeted whole-cell recordings in the mammalian brain in vivo. *Neuron* **39:** 911–918.

Nevian T, Helmchen F. 2007. Calcium indicator loading of neurons using single-cell electroporation. *Pflügers Arch* **454:** 675–688.

Rochefort NL, Garaschuk O, Milos RI, Narushima M, Marandi N, Pichler B, Kovalchuk Y, Konnerth A. 2009. Sparsification of neuronal activity in the visual cortex at eye-opening. *Proc Natl Acad Sci* **106:** 15049–15054.

Schultz SR, Kitamura K, Post-Uiterweer A, Krupic J, Häusser M. 2009. Spatial pattern coding of sensory information by climbing fiber-evoked calcium signals in networks of neighboring cerebellar Purkinje cells. *J Neurosci* **29:** 8005–8015.

Stosiek C, Garaschuk O, Holthoff K, Konnerth A. 2003. In vivo two-photon calcium imaging of neuronal networks. *Proc Natl Acad Sci* **100:** 7319–7324.

Svoboda K, Denk W, Kleinfeld D, Tank DW. 1997. In vivo dendritic calcium dynamics in neocortical pyramidal neurons. *Nature* **385:** 161–165.

Theer P, Denk W. 2006. On the fundamental imaging-depth limit in two-photon microscopy. *J Opt Soc Am A Opt Image Sci Vis* **23:** 3139–3149.

Theer P, Hasan MT, Denk W. 2003. Two-photon imaging to a depth of 1000 μm in living brains by use of a $Ti:Al_2O_3$ regenerative amplifier. *Opt Lett* **28:** 1022–1024.

Tian L, Hires SA, Mao T, Huber D, Chiappe ME, Chalasani SH, Petreanu L, Akerboom J, McKinney SA, Schreiter ER, et al. 2009. Imaging neural activity in worms, flies and mice with improved GCaMP calcium indicators. *Nat Methods* **6:** 875–881.

Tsai PS, Nishimura N, Yoder EJ, Dolnick EM, White GA, Kleinfeld D. 2002. Principles, design and construction of a two-photon laser-scanning microscope for in vitro and in vivo brain imaging. In *In vivo optical imaging of brain function* (ed. RD Frostig), pp. 113–171. CRC Press, Boca Raton, FL.

Vogelstein JT, Watson BO, Packer AM, Yuste R, Jedynak B, Paninski L. 2009. Spike inference from calcium imaging using sequential Monte Carlo methods. *Biophys J* **97:** 636–655.

Wallace DJ, Meyer zum Alten Borgloh S, Astori S, Yang Y, Bausen M, Kügler S, Palmer AE, Tsien RY, Sprengel R, Kerr JN, et al. 2008. Single-spike detection in vitro and in vivo with a genetic Ca^{2+} sensor. *Nat Methods* **5:** 797–804.

Waters J, Larkum M, Sakmann B, Helmchen F. 2003. Supralinear Ca^{2+} influx into dendritic tufts of layer 2/3 neocortical pyramidal neurons in vitro and in vivo. *J Neurosci* **23:** 8558–8567.

Yaksi E, Friedrich RW. 2006. Reconstruction of firing rate changes across neuronal populations by temporally deconvolved Ca^{2+} imaging. *Nat Methods* **3:** 377–383.

Cold Spring Harbor Protocols

www.cshprotocols.org